Mixed lineage kinase 3 inhibition induces T cell activation and cytotoxicity

Sandeep Kumar[a], Sunil Kumar Singh[a], Navin Viswakarma[a], Gautam Sondarva[a], Rakesh Sathish Nair[a], Periannan Sethupathi[a], Subhash C. Sinha[b], Rajyasree Emmadi[c], Kent Hoskins[d], Oana Danciu[d], Gregory R. J. Thatcher[e], Basabi Rana[a,f,g], and Ajay Rana[a,f,g,1]

[a]Department of Surgery, Division of Surgical Oncology, University of Illinois at Chicago, Chicago, IL 60612; [b]Laboratory of Molecular and Cellular Neuroscience, The Rockefeller University, New York, NY 10065; [c]Department of Pathology, College of Medicine, University of Illinois at Chicago, Chicago, IL 60612; [d]Division of Hematology/Oncology, College of Medicine, University of Illinois at Chicago, Chicago, IL 60612; [e]Department of Medicinal Chemistry and Pharmacognosy, University of Illinois at Chicago, Chicago, IL 60612; [f]University of Illinois Hospital and Health Sciences System Cancer Center, University of Illinois at Chicago, Chicago, IL 60612; and [g]Research Unit, Jesse Brown VA Medical Center, Chicago, IL 60612

Edited by Michael Karin, University of California San Diego School of Medicine, La Jolla, CA, and approved February 26, 2020 (received for review December 5, 2019)

Mixed lineage kinase 3 (MLK3), also known as MAP3K11, was initially identified in a megakaryocytic cell line and is an emerging therapeutic target in cancer, yet its role in immune cells is not known. Here, we report that loss or pharmacological inhibition of MLK3 promotes activation and cytotoxicity of T cells. MLK3 is abundantly expressed in T cells, and its loss alters serum chemokines, cytokines, and CD28 protein expression on T cells and its subsets. MLK3 loss or pharmacological inhibition induces activation of T cells in in vitro, ex vivo, and in vivo conditions, irrespective of T cell activating agents. Conversely, overexpression of MLK3 decreases T cell activation. Mechanistically, loss or inhibition of MLK3 down-regulates expression of a prolyl-isomerase, Ppia, which is directly phosphorylated by MLK3 to increase its isomerase activity. Moreover, MLK3 also phosphorylates nuclear factor of activated T cells 1 (NFATc1) and regulates its nuclear translocation via interaction with Ppia, and this regulates T cell effector function. In an immune-competent mouse model of breast cancer, MLK3 inhibitor increases Granzyme B-positive CD8$^+$ T cells and decreases MLK3 and Ppia gene expression in tumor-infiltrating T cells. Likewise, the MLK3 inhibitor in pan T cells, isolated from breast cancer patients, also increases cytotoxic CD8$^+$ T cells. These results collectively demonstrate that MLK3 plays an important role in T cell biology, and targeting MLK3 could serve as a potential therapeutic intervention via increasing T cell cytotoxicity in cancer.

MLK3 | CD8+ T cell | T cell activation | cytotoxic T cell | breast cancer

The mixed lineage kinases (MLKs) are distinct members of the MAP3K family due to the presence of both Ser/Thr and tyrosine kinase signature sequences within their catalytic domains (1). So far, biochemical studies have demonstrated that the MLKs are functional Ser/Thr kinases; however, their tyrosine kinase activity is still unknown (1). There are nine MLK family members that are divided into three subgroups based on characteristic structural domains (1). However, most reports related to the biology of the MLK family are described with a well-characterized MLK family member, MLK3, also known as MAP3K11 (2–4).

The detailed biological functions of MLK family members are still not well understood; however, a pan-MLK inhibitor, CEP-1347, has gone through clinical trials for Parkinson's diseases (5, 6). In addition, an MLK3-specific inhibitor, URMC-099, has shown efficacy in animal models of HIV-associated dementia (7) and in diet-induced nonalcoholic steatohepatitis (8). The URMC-099 has also shown efficacy in amyloid-β clearance in a murine model of Alzheimer's disease (9) and prevented loss of hippocampal synapses in experimental autoimmune encephalomyelitis (10). These reports clearly indicate the importance of MLK family members in a variety of neurologic conditions, yet their role in other diseases, including cancer, is not fully understood.

We have reported that MLK3 plays an important role in breast cancer. We demonstrated that MLK3 activity is necessary for the cytotoxic effects of chemotherapeutic agents in estrogen receptor-positive (ER$^+$) breast cancer (3). We also reported that MLK3 is inhibited by human epidermal growth factor receptor 2 (HER2) amplification, and this allows HER2+ breast cancer cells to proliferate and survive (11). In earlier work, we showed that cell migration is dependent on MLK3/MLKs activation and that pharmacological inhibition of MLK3/MLKs with CEP-1347 prevents breast cancer cell migration (12). These results collectively provide convincing evidence that MLKs/MLK3 are viable therapeutic targets in cancer and neurological disorders. However, the full range of functions of the MLKs in cancer is unknown. One important unexplored aspect with potential therapeutic implications is the effect of the MLKs on host immunity.

The MLK family members are reported to activate mitogen-activated protein kinase (MAPK) pathways (1, 2, 13, 14), and interestingly, MAPKs regulate a broad range of T cell functions including early thymocyte development (15); positive and negative selection of thymocytes (16); and T cell activation, differentiation, and proinflammatory responses (17–19). MAPKs also play important roles in recognition of the T cell receptor (TCR) major histocompatibility (MHC) complex and costimulatory signaling (20). T cell-specific p38 MAPK activation is reported as a component of TCR downstream signaling pathway (18), and

Significance

The agents that inhibit mitogen-activated protein kinases (MAPKs) are reported to have antineoplastic efficacies; however, their impact on immune cells is not clearly defined. We identified that genetic loss/inhibition of a MAP3K member, MLK3, increases CD8$^+$ T cell cytotoxicity via inhibition of a prolyl isomerase, Ppia, and nuclear translocation of NFATc1. The MLK3 inhibitor increased the tumor infiltration of cytotoxic T cells in an immune-competent mouse model of breast cancer. Similarly, the MLK3 inhibitor increased the cytotoxic T cell population in pan T cells isolated from breast cancer patients with metastatic disease. These results suggest that small-molecule inhibitor of MLK3 might have clinical usage even in the advanced stage of the disease, where tumor-induced immunosuppression is frequent.

Author contributions: S.K. and A.R. designed research; S.K., S.K.S., N.V., and A.R. performed research; G.S., R.S.N., P.S., and S.C.S. contributed new reagents/analytic tools; S.K., R.E., K.H., O.D., G.R.J.T., B.R., and A.R. analyzed data; S.K. and A.R. wrote the paper.

The authors declare no competing interest.

This article is a PNAS Direct Submission.

[1]To whom correspondence may be addressed. Email: arana@uic.edu.

This article contains supporting information online at https://www.pnas.org/lookup/suppl/doi:10.1073/pnas.1921325117/-/DCSupplemental.

First published March 24, 2020.

Jun N-terminal kinase (JNK) activation is reported to regulate interleukin 2 (IL2) production (21), which is necessary for T cell activation. Importantly, JNK activation plays a differential role in regulating IL2 in $CD4^+$ and $CD8^+$ T cells. The loss of JNK2 promotes IL2 production and proliferation of $CD8^+$ T cells; however, loss of JNK1 or JNK2 does not affect IL2 production or proliferation in $CD4^+$ T cells (22, 23). These reports suggest that members of the MAPK family play important roles in T cell function, and targeting these kinases may represent an approach to influence T cell activation and cytotoxicity during cancer immunotherapy.

Here we report the immune functions of MLK3, which we identified as the major MLK member present in T cells. Our results demonstrate that genetic loss or pharmacological inhibition of MLK3 promotes T cell activation and cytotoxicity. We also demonstrate that the function of MLK3 in T cells is mediated via direct phosphorylation of a Peptidyl-prolyl cis-trans isomerase A, Ppia, that regulates T cell cytotoxicity via nuclear factor of activated T cells 1 (NFATc1) nuclear translocation. Interestingly, inhibition of MLK3 leads to increased infiltration of cytotoxic $CD8^+$ T cells in a murine model of breast cancer. The MLK3 inhibition-mediated $CD8^+$ T cell cytotoxicity observed in animal and in vitro models is also replicated in $CD8^+$ T cells from breast cancer patients. Combined, these data suggest that the MLK3/Ppia/NFATc1 axis could be an important driver of the $CD8^+$ T cell cytotoxicity, and the agents targeting MLK3, such as URMC-099, warrant consideration in the management of breast or other cancer.

Results

Genetic Loss of MLK3 Promotes T Cell Activation. The role of MLK members in T cell biology is practically lacking. Therefore, first, we examined messenger RNA (mRNA) expression of all four MLK members (see primers, *SI Appendix*, Table S1) in mouse $CD4^+$ and $CD8^+$ T cells. The MLK members were differentially expressed in $CD4^+$ and $CD8^+$ T cells, and the expression of MLK3 was comparatively highest in these cells (Fig. 1 *A* and *B*). The MLK3 protein expression by Western blotting (Fig. 1*C*) and confocal microscopy (Fig. 1*D*) also showed its expression in $CD4^+$ and $CD8^+$ T cells. MLK3 expressed robustly in T cells, and therefore to determine its possible role in any immune modulation, we estimated the levels of chemokines and Th1/Th2/Th17 cytokines in sera of wild-type (WT) and MLK3 knockout (i.e., $MLK3^{-/-}$) mice. The levels of chemokines CTACK, CXCL16, CXCL1, and CCL22 were increased, whereas the levels of CCL21, CCL11, CX3CL1, IL-16, CCL8, CCL12, and CXCL12 were decreased in sera of $MLK3^{-/-}$ compared to WT mice (Fig. 1*E* and *SI Appendix*, Fig. S1). We also measured circulating cytokine levels in $MLK3^{-/-}$ and WT mice. The serum levels of cytokines IL-4 and IL-12 were comparatively higher in $MLK3^{-/-}$ mice (Fig. 1*F*). The alteration in circulating cytokines and chemokines levels due to systemic loss of MLK3 suggested a possible function of MLK3 in regulating immune cells. The surface expressions of receptors/ligands play important roles in immune cells' homeostasis, and therefore, we determined the expression of various surface molecules on splenocytes from WT and $MLK3^{-/-}$ mice. The expression of several surface molecules, especially CD28 and CD40L, were significantly up-regulated in splenocytes from $MLK3^{-/-}$ mice (*SI Appendix*, Table S2). Since IL4 and IL12 cytokines and surface molecules CD28 and CD40L were up-regulated in $MLK3^{-/-}$ mice, and these are associated with T cell activation, we sought to know whether loss of MLK3 would alter T cell activation. We measured CD28 expressions on T cells and their subsets, derived from WT and $MLK3^{-/-}$ mice. The expression of CD28 was indeed increased on T cells and their subsets, isolated from $MLK3^{-/-}$ mice (Fig. 1*G*). To understand the direct role of MLK3 in T cell activation, we then used various in vitro and in vivo approaches to activate T cells from WT and $MLK3^{-/-}$ mice. Activation of splenocytes with phytohemagglutinin-L (PHA-L) for 24 h increased the activation of T cells, as marked by increased expressions of CD25 (*SI Appendix*, Fig. S2*A*) and CD38 (*SI Appendix*, Fig. S2*C*) on $CD8^+$ T cells from $MLK3^{-/-}$ mice. Importantly, the activation of $CD8^+$ T cells was significantly higher compared to $CD4^+$ T cells from $MLK3^{-/-}$ mice (*SI Appendix*, Fig. S2 *B* and *D*). To further support the role of MLK3 in T cell activation, the splenocytes derived from WT and $MLK3^{-/-}$ mice were activated with phorbol 12-myristate–13-acetate (PMA)/ionomycin (6 h) and analyzed by flow cytometry. The percentages of $CD4^+CD25^+$ and $CD8^+CD25^+$ T cell populations were increased in absence of MLK3 (Fig. 2 *A* and *B*). We also activated purified pan T cells with antibiotin MACSiBead particles, loaded with biotinylated, anti-CD3, and anti-CD28 antibodies for 40 h. The expressions of T cell activation markers CD25 (Fig. 2 *C* and *D*) and CD69 (*SI Appendix*, Fig. S2 *E* and *F*) were increased on $CD4^+$ and $CD8^+$ T cells from $MLK3^{-/-}$ mice, compared to WT. Moreover, the T cells were activated in vivo using lipopolysaccharide (LPS), an ubiquitous immunogen present on Gram-negative bacterial membrane (24). The administration of a single dose of LPS for 2 h increased the activation of $CD4^+$ and $CD8^+$ T cells in $MLK3^{-/-}$ mice (Fig. 2 *E*–*G*). In order to complement our observation that loss of MLK3 promotes T cell activation, we established a Jurkat T cell line with stable overexpression of MLK3 (i.e., MLK3 [WT] Jurkat cells) (Fig. 2*H*). The control (vector-expressing) and MLK3 (WT) expressing Jurkat cell lines were activated with ImmunoCult (containing anti-CD3ε and anti-CD28 antibodies) for 72 h. The expressions of activation markers CD38 and CD69 were decreased in Jurkat cell line overexpressing MLK3 (Fig. 2 *I* and *J*). Taken together, these results suggest that loss of MLK3 induces T cell activation.

MLK3 Regulates Peptidyl-Prolyl Cis-Trans Isomerase A in T Cells. Our results so far suggested that MLK3 plays an inhibitory role in T cell activation, yet the mechanism(s) by which MLK3 inhibits T cell function is not known. To identify the target(s) that could mediate functional inhibition of T cells via MLK3, proteins from WT and $MLK3^{-/-}$ splenocytes were analyzed by two-dimensional (2D) difference gel electrophoresis (DIGE). The expression of at least 38 proteins was differentially regulated, including down-regulation of 11 proteins and up-regulation of 27 proteins (threshold fold change ≥ 1.4) in $MLK3^{-/-}$ compared to WT splenocytes (Fig. 3*A*). We characterized 13 differentially regulated proteins with matrix-assisted laser desorption/ionization time-of-flight/time-of-flight tandem mass spectrometry (MALDI-TOF/TOF) followed by standard bioinformatics analysis on one species against National Center for Biotechnology Information (NCBI) or SwissProt database using MASCOT software. The mass-spectroscopy analyses identified RBMXL-1, Chil3, Ahsa-1, Actg, Anxa2, Hprt1, Ngp, Camp, Cofilin-1, Peptidyl-prolyl cis-trans isomerase A (Ppia), S100a9 (two spots), and pfn1 (Fig. 3*A* and *SI Appendix*, Table S3), which were differentially expressed in splenocytes from WT and $MLK3^{-/-}$. Since we observed a 4.1-fold decrease in Ppia in splenocytes from $MLK3^{-/-}$ mice and Ppia has been implicated in T cell activation (25), we further explored the role of Ppia in MLK3-mediated T cell function. First, we determined the expression of Ppia in $CD4^+$ and $CD8^+$ T cells from WT and $MLK3^{-/-}$ mice, where Ppia protein expression in both $CD4^+$ and $CD8^+$ T cells from $MLK3^{-/-}$ mice was decreased (Fig. 3*B*). Since Ppia protein expression was significantly decreased in $MLK3^{-/-}$ T cells, we wanted to know whether Ppia protein expression could be regulated by MLK3. The Ppia protein expression was increased in Jurkat cells overexpressing WT MLK3 compared to vector control (Fig. 3*C*). MLK3 is a potent activator of JNK pathway (2), and JNK is reported to regulate gene expression via phosphorylation of AP-1 transcription factor (21). In silico promoter analysis of Ppia revealed at least four conserved putative AP-1 binding sites (*SI*

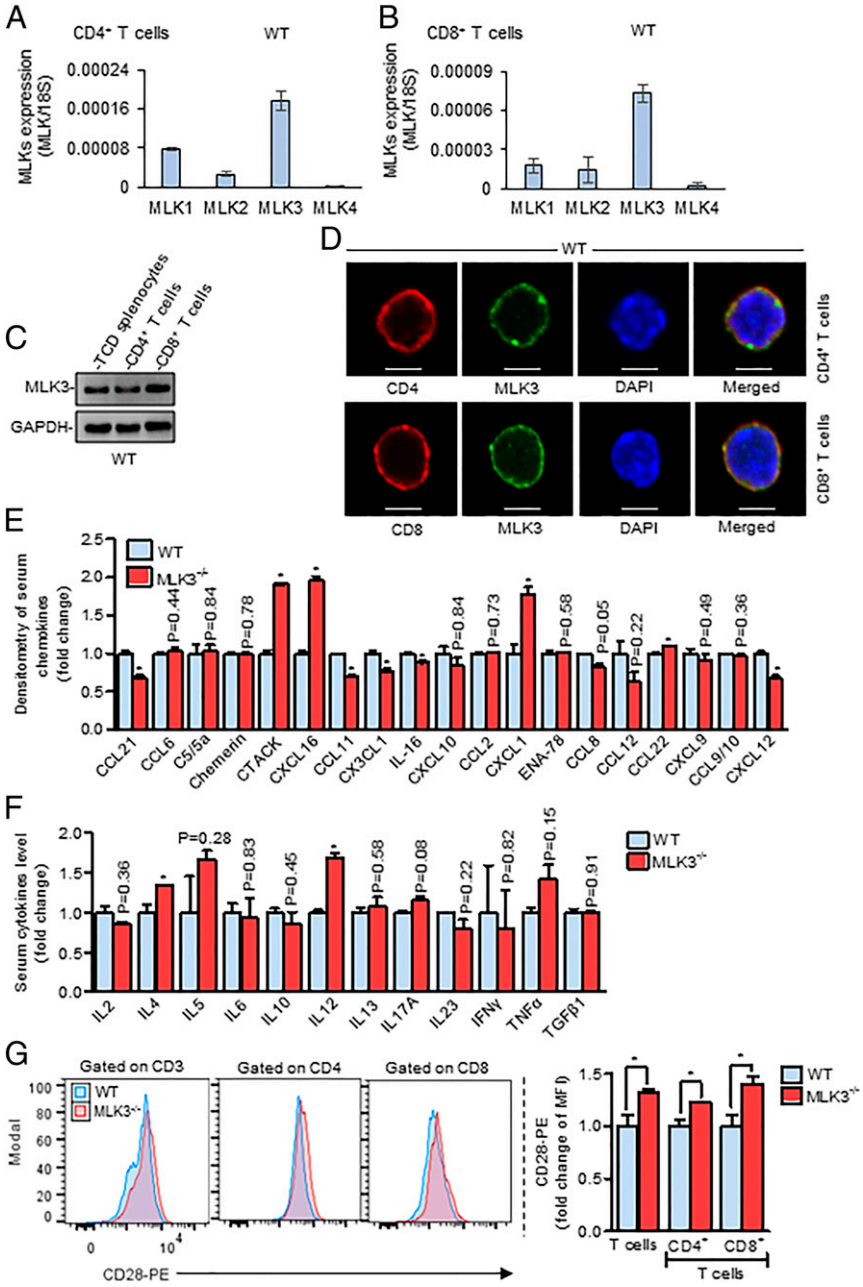

Fig. 1. Loss of MLK3 induces immune modulation. (*A* and *B*) Expressions of *MLK1*, *MLK2*, *MLK3*, and *MLK4* mRNA in $CD4^+$ and $CD8^+$ T cells, determined by qPCR. $n = 2$ mice per group. (*C*) Western blot of MLK3 protein expression in T cell-depleted (TCD) splenocytes, $CD4^+$ and $CD8^+$, T cells total lysates. Immunoblot was performed with the MLK3 specific antibody, and GAPDH was used as loading control. A representative experiment out of two has been presented. (*D*) Pan T cells were isolated from WT and $MLK3^{-/-}$ mice and cytospin on glass slides. The cells were stained either with anti-CD4 and MLK3 antibodies or anti-CD8 and MLK3 antibodies, respectively. DAPI was used for nuclear staining (scale bar, 5 μm). A representative experiment out of two has been presented. (*E*) Quantification of the serum chemokine profile shown by proteome profiler array. Pooled sera, $n = 3$ mice per group. (*F*) Serum Th1/Th2/Th17 cytokines quantification by enzyme-linked immunosorbent assay (ELISA) (pooled sera, $n = 5$ mice per group; technical replicates). (*G*) Histogram plots of CD28 expression (*Left*) on T cells and its subsets and quantification (*Right*) shown by flow cytometry, $n = 3$ mice per group. MFI, mean fluorescence intensity. Quantitative data in all panels are means ± SD. $^*P < 0.05$ (unpaired two-tailed Student's *t* test). The experiment of *A*–*D* and *G* was repeated at least twice.

Appendix, Table S4), suggesting that Ppia gene expression might be regulated via the MLK3-JNK-AP-1 axis. The Jurkat cells expressing WT MLK3 (i.e., MLK3 [WT]) were treated with an AP-1/c-Fos inhibitor, T-5224 (26), for 24 h, and gene expression of Ppia was estimated. Indeed, the gene expression of Ppia was significantly down-regulated upon T-5224 treatment (Fig. 3*D*).

The prolyl isomerases are reported to be regulated via phosphorylation (27), and therefore, we examined any possible interaction between MLK3 and Ppia in activated T cells by using a proximity ligation assay (PLA). The MLK3-Ppia PLA blobs were observed; however, their numbers were limited in activated T cells (*SI Appendix*, Fig. S3*A*). The MLK3-Ppia PLA blobs were limited in activated T cells, and thus, we determined the interaction between Ppia and MLK3 in purified $CD8^+$ T cells under basal condition. The interaction was stronger under basal conditions, and several positive MLK3-Ppia PLA blobs were observed in $CD8^+$ T cells (Fig. 3*E*). The interaction between MLK3 and Ppia was also

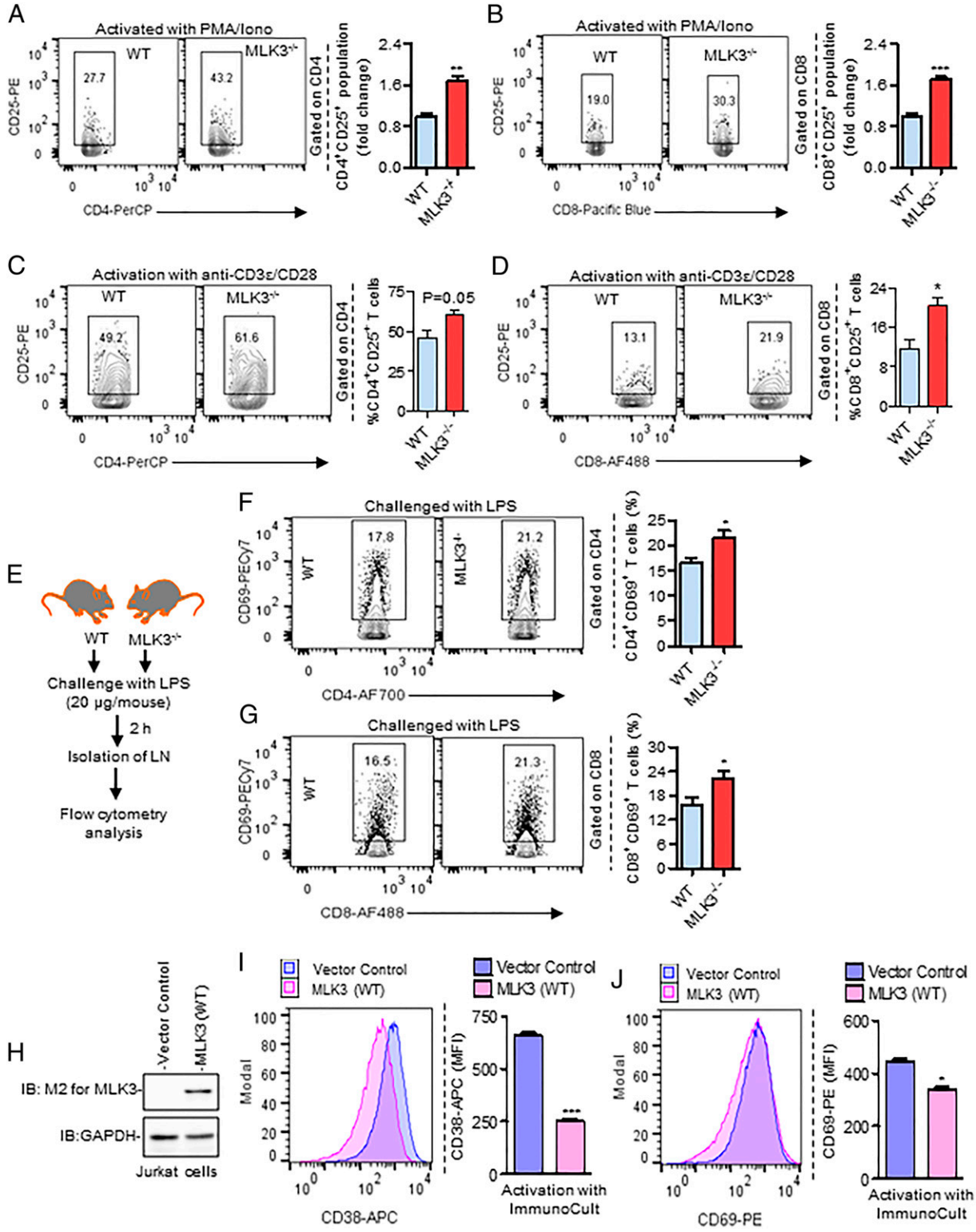

Fig. 2. Loss of MLK3 induces T cell activation. (*A* and *B*) Splenocytes from WT and MLK3$^{-/-}$ mice were activated with PMA/ionomycin (6 h), and expressions of CD25 on CD4$^+$ and CD8$^+$ T cells were analyzed by flow cytometry. *A* and *B* are representative contour plots of CD4 or CD8 versus CD25 (*Left*) and quantification (*Right*). $n = 4$ mice per group; quantitative data are means ± SD. (*C* and *D*) Representative contour plots of CD25 on CD4$^+$ and CD8$^+$ T cells (*Left*) and quantification (*Right*) by flow cytometry after 40 h activation with indicated agents. $n = 4$ mice per group; quantitative data are means ± SEM. (*E–G*) WT and MLK3$^{-/-}$ mice were treated with LPS (2 h), and expressions of CD69 on CD4$^+$ and CD8$^+$ T cells isolated from lymph nodes (LN) population were analyzed. *F* and *G* show representative contour plots of CD69 on CD4$^+$ and CD8$^+$ T cells (*Left*) and quantification (*Right*). $n = 5$ mice per group, quantitative data are means ± SEM. (*H*) Western blot of M2-MLK3 in total lysates of vector control and MLK3 (WT) Jurkat cells. Immunoblot was performed with the M2 specific antibody, and GAPDH was used as loading control. A representative experiment out of two has been presented. (*I* and *J*) Representative histogram plots of CD38 and CD69 expression (*Left*) and quantification (*Right*) by flow cytometry after 72 h of activation with ImmunoCult (containing anti-CD3ε and anti-CD28 antibodies). $n = 3$; quantitative data are means ± SEM. *$P < 0.05$, **$P < 0.01$, and ***$P < 0.0001$ (unpaired two-tailed Student's *t* test). All experiments were repeated at least twice.

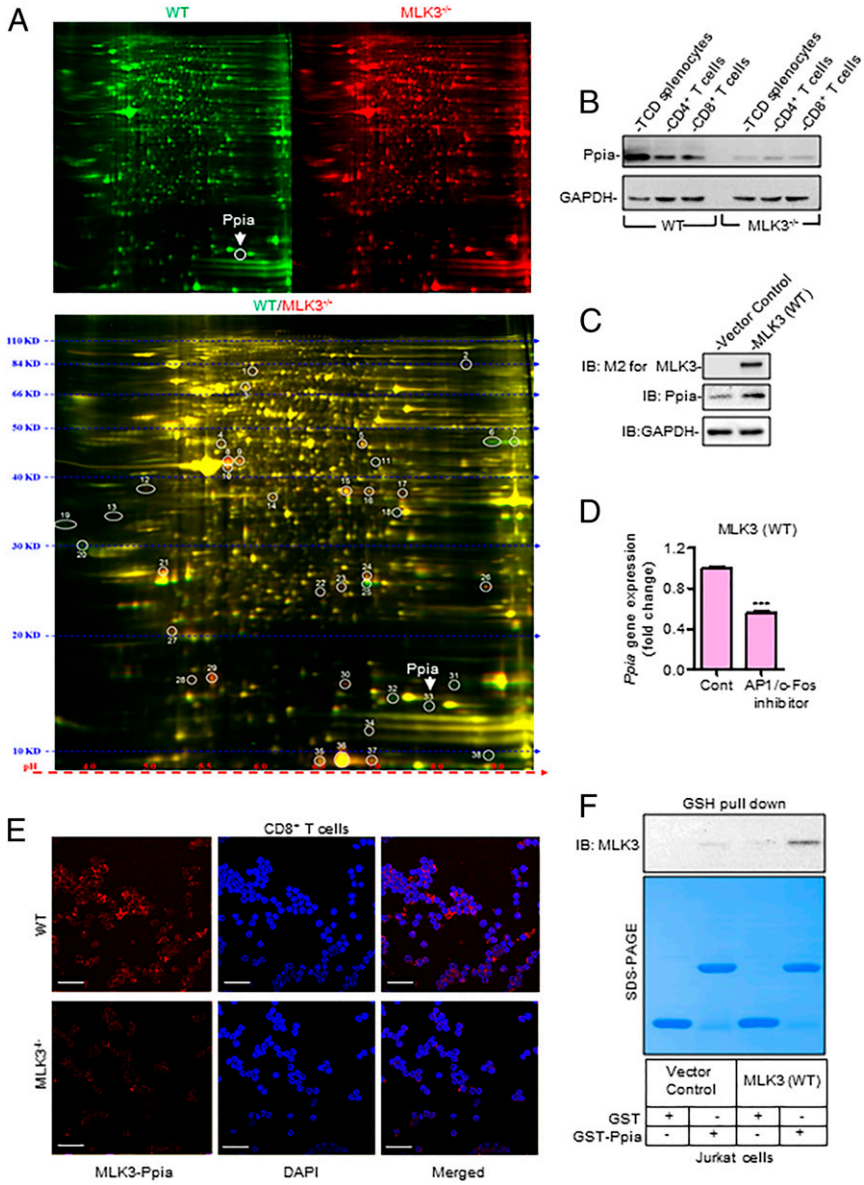

Fig. 3. MLK3 regulates peptidyl-prolyl cis-trans isomerase A (Ppia) in T cells. (*A*) Two-dimensional difference gel electrophoresis (2D-DIGE) of splenic protein lysates from WT and MLK3$^{-/-}$ mice. Pooled, $n = 3$ mice per group. (*B*) Western blot of Ppia protein expression in TCD splenocytes, CD4$^+$ and CD8$^+$, T cells total lysates. Immunoblot was performed with the Ppia specific antibody. (*C*) Western blot of Ppia in total lysates of vector control and MLK3 (WT) Jurkat cells. Antibodies were used as indicated. (*D*) *Ppia* gene expression in MLK3 (WT) Jurkat cells in absence and presence of AP1/cFos inhibitor (T5224) as determined by qPCR. As an internal control, 18S rRNA was used. $n = 3$; quantitative data are means ± SD. ***$P < 0.0001$ (unpaired two-tailed Student's *t* test). (*E*) Representative images of proximity ligation assay (PLA) for MLK3-Ppia in CD8$^+$ T cells under basal condition (scale bar, 20 μm). (*F*) GSH pulldown assay for interaction between MLK3 and Ppia using total lysates of vector control and MLK3 (WT) Jurkat cells. The experiments of *C*–*F* were repeated twice.

determined in MLK3 (WT) expressing Jurkat T cells by MLK3 pulled down with bacterially expressed GST-tagged recombinant Ppia. The recombinant Ppia was able to pull down MLK3 (Fig. 3*F*), suggesting that MLK3 binds with Ppia. Earlier, we reported that MLK3 phosphorylates prolyl-isomerase, Pin1, and this phosphorylation increased the catalytic activity of Pin1 (2, 4), and therefore, we examined whether Ppia can also be phosphorylated by MLK3 to increase its isomerase activity. The bacterially expressed Ppia protein was indeed directly phosphorylated by MLK3 enzyme (Fig. 4*A*), and isomerase activity of Ppia was increased upon MLK3-induced phosphorylation (Fig. 4*B*). These results collectively suggest that Ppia's expressions, phosphorylation, and cis trans isomerase activity in T cells are regulated by MLK3.

MLK3-Ppia Axis Regulates NFATc1 Nuclear Translocation and T Cell Effector Function. We observed above that T cells from MLK3$^{-/-}$ mice were hyperactivated compared to WT mice, and Ppia protein was decreased in T cells from MLK3$^{-/-}$ mice. These results suggest that perhaps MLK3-dependent Ppia protein expression might influence T cell effector function. It is reported that loss of Ppia in T cells increases NFAT's DNA-binding activity and, thus, T cell function (25). To understand the role of MLK3-regulated Ppia in NFATc1-mediated T cell function, we first examined any possible interaction between Ppia and NFATc1 by PLA in CD8$^+$ T cells, derived from WT and MLK3$^{-/-}$ mice. The PLA results showed a possible interaction between MLK3-regulated Ppia and NFATc1 in CD8$^+$ T cells (Fig. 4*C*). Importantly, the NFATc1-Ppia blobs were restricted to cytosol in CD8$^+$ T cells from WT mice (Fig. 4*C*).

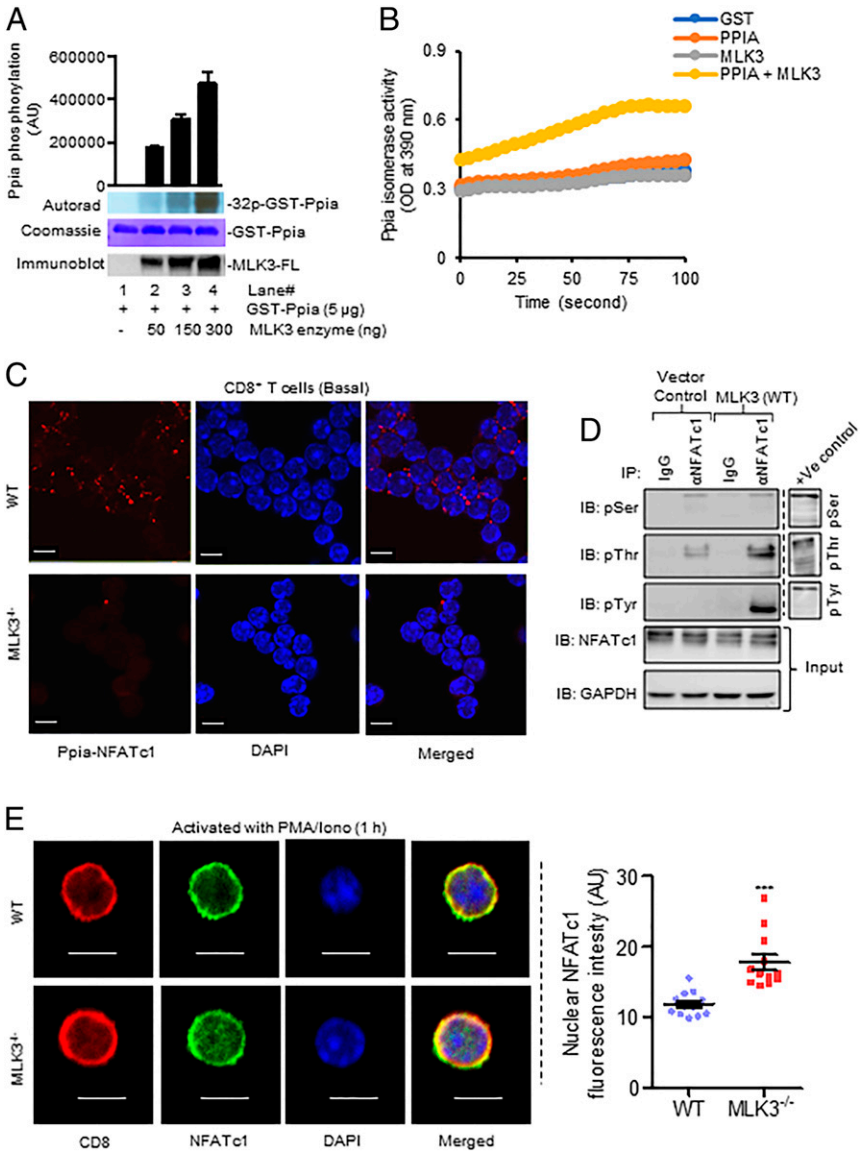

Fig. 4. MLK3 phosphorylates Ppia and increases nuclear translocation of NFATc1. (*A*) Phosphorylation of Ppia protein by MLK3 enzyme by using in vitro kinase assay. Quantitative data are means ± SEM. A representative experiment out of two has been presented. (*B*) In vitro assay for Ppia cis-trans isomerase activity. Enzyme kinetics were recorded at 390 nm. A representative experiment out of two has been presented. (*C*) Representative PLA images of Ppia-NFATc1 in $CD8^+$ T cells from WT and $MLK3^{-/-}$ mice (scale bar, 5 μm). $n = 3$ mice per group. (*D*) Immunoprecipitation (IP) of NFATc1 from total protein lysates of vector control and MLK3 (WT) Jurkat cells followed by immunoblotting (IB) with phospho serine (pSer), phospho threonine (pThr), and phospho tyrosine (pTyr) specific antibodies. Mouse brain lysate for pSer and sorbitol-treated HEK-293 cell lysate for pThr and pTyr were used as controls. A representative experiment out of two has been presented. (*E*) Representative confocal images of NFATc1 in $CD8^+$ T cells from WT and $MLK3^{-/-}$ after 1 h of activation with PMA/ionomycin. Quantification by Image J, $n = 12$ cells per group (scale bar, 5 μm). Quantitative data are means ± SEM. $^{***}P < 0.0001$ (unpaired two-tailed Student's *t* test).

We also determined possible interaction between NFATc1 and Ppia in activated Jurkat cell lines, and, indeed, the number of NFATc1-Ppia blobs were significantly higher in cells overexpressing MLK3 (*SI Appendix*, Fig. S3*B*). The NFAT nuclear translocation and function are regulated via phosphorylation–dephosphorylation mechanisms, where phosphorylation prevents and dephosphorylation promotes its nuclear translocation (28). To determine whether MLK3 could regulate NFATc1 nuclear translocation via phosphorylation, we first examined the phosphorylation status of NFATc1 in Jurkat T cell lines, either expressing MLK3 (WT) or vector control. The NFATc1 phosphorylation on Thr and Tyr but not on Ser residues was increased in Jurkat cells expressing WT MLK3 (Fig. 4*D*), indicating that MLK3 could regulate translocation of NFATc1. NFATc1 was phosphorylated in MLK3-expressing Jurkat T cells, and phosphorylated NFATc1 is retained in cytoplasm, and therefore, we asked whether loss of MLK3 could promote NFATc1 nuclear translocation. The localization of NFATc1 in PMA/ionomycin-activated $CD8^+$ and $CD4^+$ T cells from WT and $MLK3^{-/-}$ was analyzed by confocal microscopy. The NFATc1 was primarily nuclear in $CD8^+$ (Fig. 4*E*) and $CD4^+$ T cells, isolated from $MLK3^{-/-}$ mice (*SI Appendix*, Fig. S4). Since Ppia expression was regulated by MLK3, and it is reported that loss of Ppia increases the transcriptional activity of NFAT (25), we determined the role of MLK3-regulated Ppia on nuclear translocation of NFATc1. The vector control and MLK3 (WT) expressing Jurkat cells were activated with PMA/ionomycin, and expression of Ppia and NFATc1 nuclear localization were determined by microscopy. The nuclear translocation of NFATc1 in MLK3 (WT) Jurkat cells was

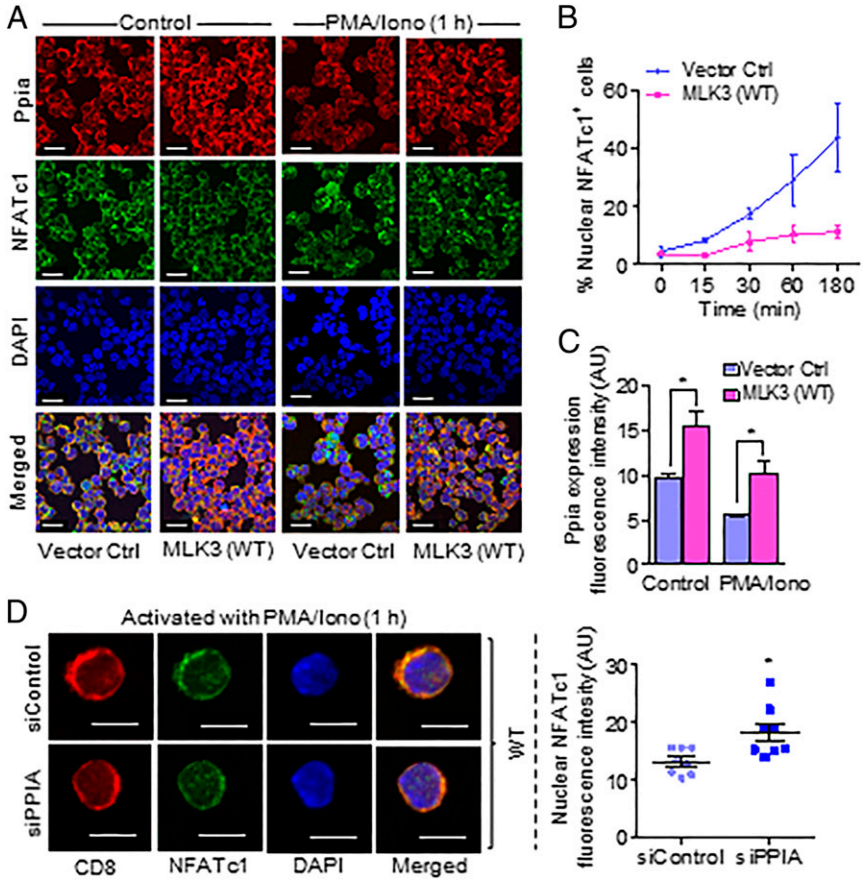

Fig. 5. Nuclear translocation of NFATc1 is regulated via MLK3-Ppia axis. (*A*) Representative confocal images of Ppia and NFATc1 in vector ctrl (control) and MLK3 (WT) Jurkat cells activated with PMA/Ionomycin (1 h); $n = 3$ (scale bar, 20 μm). (*B*) Vector control and MLK3 (WT) Jurkat cells were activated for indicated time periods, and immunofluorescence images were quantified for nuclear NFATc1 expression using Image J software; $n = 3$, quantitative data are means ± SEM. (*C*) Quantification of Ppia expression in control and MLK3 (WT) Jurkat cells from experiment of *A*; $n = 3$, quantification by Image J; quantitative data are means ± SEM. (*D*) Pan T cells were transfected either with *Ppia* specific small interfering RNA (siRNA) (siPpia) or scrambled siRNA (siControl) and activated for 1 h. *D* shows representative images of NFATc1 in $CD8^+$ T cells; quantification by Image J, $n = 8$ cells per group (scale bar, 5 μm); quantitative data are means ± SEM. $^*P < 0.05$ (unpaired two-tailed Student's *t* test). The experiments of *A*–*C* were repeated at least twice.

attenuated at all time points of activation and correlated with increased expression of Ppia (Fig. 5 *A*–*C*). To determine whether MLK3-induced Ppia regulates NFATc1 nuclear translocation, the *Ppia* was knocked down in pan T cells derived from WT mice (*SI Appendix*, Fig. S5 *A* and *B*) and then activated with PMA/ionomycin. The nuclear translocation of NFATc1 was increased upon knockdown of *Ppia*, suggesting that MLK3-induced Ppia negatively regulates the nuclear translocation of NFATc1 (Fig. 5*D* and *SI Appendix*, Fig. S5*C*).

Nuclear localization of NFATc1 is reported to induce $CD8^+$ T cell cytotoxicity (29); we next examined any impact of MLK3 on cytotoxic T cell phenotypes. Flow cytometry analyses of activated pan T cells from WT and $MLK3^{-/-}$ showed a higher percentage of $CD8^+$granzyme B^+ ($CD8^+GZMB^+$) and $CD8^+IFN\gamma^+TNF\alpha^+$ T cells in absence of MLK3 (Fig. 6 *A* and *B*). We also determined cytotoxic phenotypes of $CD4^+$ T cells. Again, loss of MLK3 increased the percentage of $CD4^+GZMB^+$ and $CD4^+IFN\gamma^+TNF\alpha^+$ T cell phenotypes (*SI Appendix*, Fig. S6 *A* and *B*). To further understand the physiological relevance of MLK3 in cytotoxicity of T cells, WT and $MLK3^{-/-}$ mice were sensitized with OVA, and splenocytes (i.e., effector cells) were prepared. Next, the splenocytes from naive WT mice were pulsed either with OVA peptide, SIINFEKL, or phosphate-buffered saline (PBS) and labeled with CFSE (i.e., target cells). The effector and target cells were cocultured ex vivo, and after 12 h the total live cells (i.e., CFSE-positive) were determined after exclusion of dead cells. The OVA peptide-pulsed CFSE-positive target cells were significantly less in coculture where OVA-sensitized effector cells from $MLK3^{-/-}$ mice were used (*SI Appendix*, Fig. S7*A*). In another complementary experiment for $CD8^+$ T cell cytotoxicity, $CD8^+$ T cells from OVA-sensitized WT and $MLK3^{-/-}$ mice were purified. These $CD8^+$ T cells were cocultured with OVA peptide-pulsed, dendritic cells (DCs) from naive mice, along with CFSE-labeled E.G7-OVA cells (E.G7-OVA $CFSE^+$ cells). The flow cytometry analyses showed a decrease in live E.G7-OVA $CFSE^+$ cells in the group where $CD8^+$ T cells were derived from $MLK3^{-/-}$ mice (*SI Appendix*, Fig. S7*B*). In summary, our results demonstrate that loss of MLK3 decreases Ppia protein expression and increases NFATc1 nuclear translocation to induce $CD8^+$ T cell effector function.

Pharmacological Inhibition of MLK3 Affects T Cell Function Similar to Genetic Loss of MLK3. The small-molecule URMC-099 is reported as a specific inhibitor of MLK3 (7). We observed above that loss of MLK3 induced T cell activation and effector function. Therefore, we envisioned that pharmacological inhibitor should have a similar effect on T cell function. Splenocytes from WT (C57BL/6) mice were stimulated with PHA-L in the presence and absence of URMC-099. The URMC-099 treatment indeed enriched the population of activated $CD8^+$ T cells (i.e., $CD8^+CD38^+$ T cells) (*SI Appendix*, Fig. S8*A*), similar to loss of MLK3. We further determined the effect of URMC-099 on T cell effector function by

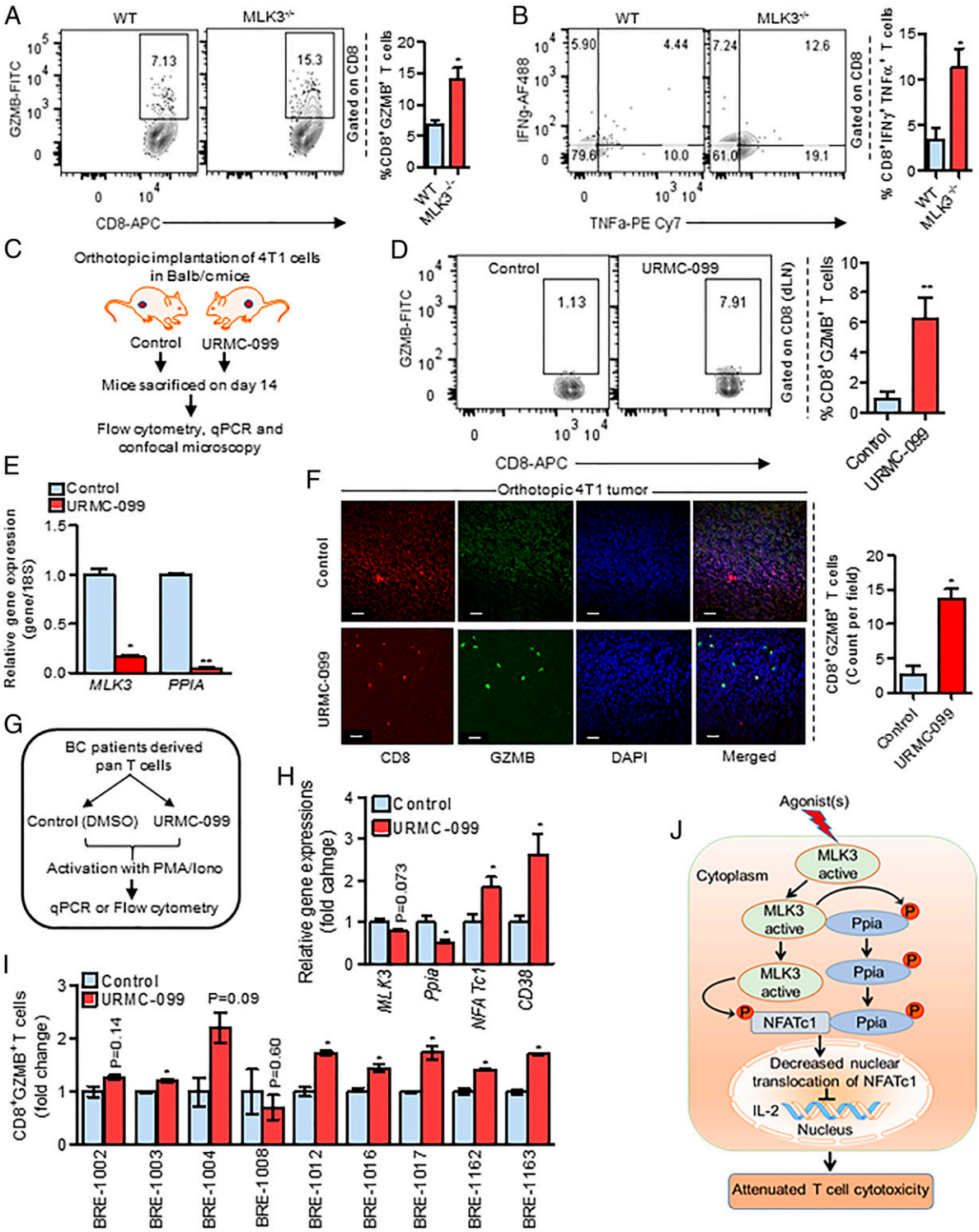

Fig. 6. Genetic loss or pharmacological inhibition of MLK3 promotes CD8$^+$ T cell cytotoxicity. (*A* and *B*) Pan T cells were activated with anti-biotin MACSiBead particles, loaded with biotinylated, anti-CD3, and anti-CD28 antibodies, and intracellular granzyme B (GZMB), IFNγ, and TNFα were determined by flow cytometry. *A* and *B* show representative contour plots of GZMB$^+$ and IFNγ$^+$TNFα$^+$; CD8$^+$ T cells (*Left*) and quantification (*Right*), $n = 3$ mice per group; quantitative data are means ± SEM (unpaired two-tailed Student's *t* test). (*C*) Experimental plan for *D*–*F*. (*D*) Representative contour plots of intracellular expression of GZMB in CD8$^+$ T cells (*Left*) in lymph nodes of control and URMC-099-treated tumor-bearing mice and quantification (*Right*); $n = 5$ mice per group, quantitative data are means ± SEM. (*E*) The qPCR analysis for *MLK3* and *Ppia* gene expressions in tumor-infiltrating T cells; $n = 2$, quantitative data are means ± SD. (*F*) Representative confocal images of GZMB expression in CD8 of tumor sections from control and URMC-099-treated group and quantification using Image J (scale bar, 20 μm); $n = 3$ mice per group, quantitative data are means ± SEM (unpaired two-tailed Student's *t* test). (*G*) Experimental plan for *H* and *I*. (*H*) Gene expressions of *MLK3* (or *MAP3K11*), *Ppia*, *NFATc1*, and *CD38* by qPCR ($n = 5$ biological, $n = 2$ technical); quantitative data are means ± SD (unpaired two-tailed Student's *t* test). (*I*) CD8$^+$GZMB$^+$ T cell population in breast cancer patients derived pan T cells shown by flow cytometry ($n = 9$ biological, $n = 2$ technical), quantitative data are means ± SD (unpaired two-tailed Student's *t* test). (*J*) Proposed model for role of MLK3 in T cell cytotoxicity. $^*P < 0.05$ and $^{**}P < 0.01$. Experiments *A*, *B*, *D*, and *F* were repeated twice.

measuring intracellular GZMB in $CD8^+$ T cells upon activation of pan T cells with PMA/ionomycin. The expression of GZMB in $CD8^+$ T cells upon treatment with URMC-099 was significantly increased (*SI Appendix*, Fig. S8*B*). To determine the in vivo effect of URMC-099 on T cell activation, C57BL/6 mice were treated with the MLK3 inhibitor (*SI Appendix*, Fig. S8*C*), and pan T cells were isolated from splenocytes of control and URMC-099–treated mice and subjected to activation with anti-biotin MACSiBead particles, loaded with biotinylated, anti-CD3, and anti-CD28 antibodies. The activation of $CD8^+$ T cells was increased in the URMC-099–treated group, as evidenced by up-regulation of the $CD8^+CD69^+$ T cell population (*SI Appendix*, Fig. S8*D*), similar to T cells from $MLK3^{-/-}$ mice.

Cytotoxic T cells are important for tumoricidal effect, and MLK3 inhibitor, URMC-099 had effect on T cells effector function, and therefore we determined the physiological relevance of MLK3 inhibition in animal model of breast cancer. We used a syngeneic mouse breast cancer cell line, 4T1, in BALB/c mice to develop orthotopic breast tumors (Fig. 6*C*). The population of $CD8^+GZMB^+$ T cells was estimated in draining lymph nodes (dLN) from tumor-bearing mice, either treated with vehicle or URMC-099. Flow cytometry analyses showed a significantly higher percentage of $CD8^+GZMB^+$ T cell population in the dLN of tumor-bearing mice treated with URMC-099 (Fig. 6*D*). We observed above that the expression of Ppia was decreased in T cells from MLK3 knockout mice, and decrease of Ppia was associated with increased T cell effector function. Therefore, we sought to determine whether MLK3 inhibitor will have a similar effect on tumor-infiltrating T cells. The *Ppia* and *MAP3K11* (*MLK3*) gene expressions in tumor-infiltrating T cells isolated from control and URMC-099–treated mice were determined. The qPCR results showed a significant decrease in *MLK3* and *Ppia* expressions in tumor-infiltrating T cells from the group treated with URMC-099 (Fig. 6*E*). In addition, we also determined GZMB expression in tumor-infiltrating $CD8^+$ T cells, and, indeed, $CD8^+$ T cells with GZMB expression were exclusively seen in the URMC-099 treatment group (Fig. 6*F*). Taken together, these results show that pharmacological inhibition of MLK3 promotes T cell activation and cytotoxicity, similar to genetic loss of MLK3.

In vitro Inhibition of MLK3 in Pan T Cells from Breast Cancer Patients Increases Cytotoxic $CD8^+$ T Cell Population. To understand the clinical significance of MLK3 in immune cell function, peripheral blood mononuclear cells (PBMCs) were isolated from female patients with advanced breast cancer (see *SI Appendix*, Table S5 for patient details). The PBMCs were cultured and treated first with MLK3 inhibitor, URMC-099, and then activated with PMA/ionomycin. The expression of several immune-related genes in PBMCs was determined using the NanoString Human Immunology panel. Normalized mRNA counts of *NFATc1*, *IL2*, *CD40LG*, and *IFNγ* were up-regulated several folds upon activation with PMA/ionomycin, in presence of URMC-099 (*SI Appendix*, Fig. S9 *A*–*C*).

We also examined the impact of MLK3 inhibition on pan T cells isolated from breast cancer patients (see *SI Appendix*, Table S5 for patient details). Pan T cells were isolated from whole blood and treated with either URMC-099 or vehicle and then activated with PMA/Ionomycin (3 h) (Fig. 6*G*). Expressions of the MLK3-regulated genes that were identified in mouse T cells were determined in pan T cells from breast cancer patients by qPCR. Similar to mouse T cells from MLK3 knockout, the expression of *Ppia* was decreased, whereas the expressions of *NFATc1* and *CD38* genes were increased in the URMC-099–treated group (Fig. 6*H*; for primers, see *SI Appendix*, Table S1). The effect of MLK3 inhibition on the cytotoxic T cell population was also determined using pan T cells from breast cancer patients. Flow cytometry analysis showed a significant increase in $CD8^+GZMB^+$ T cell population, following inhibition of MLK3 by URMC-099 (Fig. 6*I* and *SI Appendix*, Fig. S9*D*). These results collectively demonstrate that inhibition of MLK3 is also able to increase cytotoxic T cell population in blood samples from breast cancer patients.

Discussion

The considerable progress in developing targeted cancer therapies over the past few decades has focused primarily on targeting oncogenic signaling pathways. However, the effects of these therapies on the host immune system, which plays an important role in the clinical efficacy of antineoplastic therapies, are poorly understood. The MAPKs or their downstream effectors have been targeted for cancer therapy and are reported to play an important role in host immunity (30, 31). Here, we report the role of a poorly understood MAPK member, MLK3, in T cell function and its impact on host immunity. We show that inhibition of MLK3 in T cells from breast cancer patients increases the population of cytotoxic $CD8^+$ T cells, highlighting the clinical relevance of our finding.

T cell activation is a key step in the immune response and is determined by three major factors: 1) binding of TCR to MHC, 2) activation of costimulatory pathways, and 3) an immunosupportive microenvironment. Indeed, analyses of T cells from MLK3 knockout mice had higher expression of costimulatory molecules CD28 and CD40L under basal condition, corroborating one of the mechanisms by which loss of MLK3 can activate T cells. Our results show that loss of MLK3 promotes T cell activation with a broad range of stimuli, including PHA-L, PMA/ionomycin, LPS, and anti-CD3/CD28 antibodies, suggesting that MLK3 plays an important role in T cell activation, irrespective of the nature of the activating stimulus. Furthermore, we also defined in detail the mechanism of MLK3-mediated inhibition of T cell effector function. Our results show that a member of prolyl-isomerase, Ppia, is down-regulated due to loss of MLK3 in T cells. Ppia was further shown to be phosphorylated by MLK3, which plays a role in retaining NFATc1 outside the nucleus. Moreover, we observed that loss of MLK3 decreases Ppia, and this allows nuclear translocation NFATc1 for increasing T cell cytoxicity. Taken together, our data clearly showed that MLK3 negatively regulates NFATc1 nuclear translocation and effector function of T cells (Fig. 6*J*).

The small-molecule URMC-099 is reported to be a specific inhibitor of MLK3 (7). Our in vitro and in vivo results suggest that pharmacological inhibition of MLK3 with URMC-099 in mice has the same effect on T cell activation and effector function as MLK3 loss. These observations provide the foundation and strong rationale for clinical use of URMC-099 to enhance cytotoxic T cell activity as immunotherapy in cancer. In vivo results with 4T1 breast cancer orthotopic xenografts in immune-competent mouse demonstrated that inhibition of MLK3 promotes cytotoxic $CD8^+$ T cell population in draining lymph nodes as well as in tumor. T cell activation is a prerequisite for its effector function, and in the majority of cancers, the host or tumor-infiltrating T cells lack activation and therefore effector function. This creates a condition where T cells are ineffective due to T cell anergy and immune tolerance. Our results showed that pharmacological inhibition of MLK3 was able to augment effector function of both peripheral as well as tumor-infiltrating $CD8^+$ T cells. Consistent with our findings in animal models, pharmacological inhibition of MLK3 in T cells from breast cancer patients induced $CD8^+$ T cell cytotoxicity in vitro. Importantly, the pan T cells were isolated from patients with metastatic disease (i.e., stage IV). Even in the advanced disease setting, URMC-099 increased the activation and cytotoxicity of T cells, suggesting that MLK3 inhibition may have clinical benefit even in advanced stages of disease where tumor-induced immunosuppression is most profound.

In conclusion, our study elucidates a significant role of MLK3 in T cell activation and effector function. Loss of MLK3 up-regulates costimulatory molecules CD28 and down-regulates Ppia

to modulate T cell effector function via NFATc1 nuclear translocation. Based on our data and published reports, we propose that inhibition of MLK3 could serve as an immunotherapeutic approach for cancer treatment.

Materials and Methods

Human blood samples from breast cancer patients were collected upon written informed consents. Detailed information of materials and methods and associated references is available in the *SI Appendix*.

Mice and Cell Lines. The MLK3$^{-/-}$ breeding pairs in C57BL/6 background were initially obtained from Roger Davis (UMass Memorial Medical Center, Worcester, MA) and bred in-house to obtain WT and homozygous MLK3$^{-/-}$ mice. Sex- and age-matched WT and MLK3$^{-/-}$ mice (6–10 wk old) were used for experiments. The age-matched C57BL/6 mice were treated (i.p. injection) either with MLK3 inhibitor, URMC-099 (dose 7.5 mg/kg body weight), or vehicle (control) for 3 wk daily to inhibit MLK3 activity in vivo. Female BALB/c mice were obtained from Charles River Laboratory. The mice were housed in Biologic Resources Laboratory (BRL) facility on a commercial diet and water. All animal experiments were performed under a protocol approved by University of Illinois at Chicago-Institutional Animal Care and Use Committee (UIC-IACUC). Jurkat cells (clone E6-1), E.G7-OVA, and 4T1 cells were obtained from American Type Culture Collection (ATCC) and maintained according to ATCC-recommended medium supplemented with 10% heat-inactivated FBS and 100 IU/mL penicillin/streptomycin (Gibco).

Antibodies. The details of antibodies used for flow cytometry, Western blotting, and immunofluorescence are given in *SI Appendix*, Table S6.

In Vitro and In Vivo T Cell Activation. The splenocytes were stimulated using PHA-L (2.5 μg/mL; eBiosciences) and PMA/ionomycin mixture (2 μL/mL; this mixture contains phorbol-12-myristate 13-acetate [40.5 μM] and ionomycin [669.3 μM] in DMSO; BioLegend) for various time points. The pan T cells (2×10^6/well) were activated using anti-biotin MACSiBead particles, loaded with biotinylated, anti-CD3, and anti-CD28 antibodies (mouse T Cell Activation/Expansion Kit; Miltenyi Biotec) in presence of 50 U/mL of recombinant mIL-2 (BioLegend). For in vivo activation of T cells, WT and MLK3$^{-/-}$ mice were given LPS (20 μg/mouse, Sigma-Aldrich) for 2 h. Vector control and MLK3 (WT) Jurkat T cells were activated either with PMA/ionomycin or ImmunoCult human CD3/CD28 T cell activator (STEMCELL Technologies, Inc.) for different time points, as indicated.

Breast Cancer Orthotopic Model. Mouse breast cancer cell line 4T1 was used to generate orthotopic xenograft in BALB/c mice. The 4T1 cell line was authenticated by STR profiling and tested for any microbial or bacterial contamination before using in mice. The 4T1 cells (10,000 per mouse) were implanted orthotopically in mammary fat pads of female BALB/c mice (10–12 wk). The tumor-bearing mice with average tumor diameter of 5 mm (10–11 d after 4T1 inoculation) were randomized into two groups and treated as follows: group 1, vehicle control and group 2, URMC-099 (dose 7.5 mg/kg body weight daily). The treated and control mice were sacrificed on day 14, and dLN and tumors were collected for experiments.

Statistical Analyses. Statistical significance was calculated with Graph Pad Prism software. To compare two groups, data were analyzed by Student's *t* test (unpaired, two-tailed). Multiple groups were analyzed by one-way ANOVA followed by Bonferroni's multiple-comparisons test. The error bars indicate SD or SE of mean (SEM). $P < 0.05$ was considered statistically significant. * indicates $P < 0.05$; ** indicates $P < 0.01$, and *** indicates $P < 0.001$.

SI Appendix. Supplementary materials and methods, supporting figures (*SI Appendix*, Figs. S1–S9) and tables (*SI Appendix*, Tables S1–S6), and supplementary references are available in *SI Appendix*.

Data Availability. All data discussed in the paper are included in the manuscript and *SI Appendix*.

ACKNOWLEDGMENTS. We acknowledge Enrico Benedetti, M.D, Chair Department of Surgery, for providing access to departmental resources and financial support. The authors also acknowledge Ms. Janet York for her administrative support and Dr. Balaji Ganesh, director of the University of Illinois at Chicago (UIC) flow cytometer core facility, for his technical advice. We acknowledge funding support from the National Cancer Institute (Grants CA176846 and CA216410 [to A.R.] and CA178063 and CA219764 [to B.R.]). Additional support came from Veteran Administration Merit Awards and Career Scientist Award (BX002703 and BX004855 [to A.R.] and BX003296 [to B.R.]).

1. A. Rana *et al*., Mixed lineage kinase-c-Jun N-terminal kinase axis: A potential therapeutic target in cancer. *Genes Cancer* **4**, 334–341 (2013).
2. A. Rana *et al*., The mixed lineage kinase SPRK phosphorylates and activates the stress-activated protein kinase activator, SEK-1. *J. Biol. Chem.* **271**, 19025–19028 (1996).
3. V. Rangasamy *et al*., Estrogen suppresses MLK3-mediated apoptosis sensitivity in ER+ breast cancer cells. *Cancer Res.* **70**, 1731–1740 (2010).
4. V. Rangasamy *et al*., Mixed-lineage kinase 3 phosphorylates prolyl-isomerase Pin1 to regulate its nuclear translocation and cellular function. *Proc. Natl. Acad. Sci. U.S.A.* **109**, 8149–8154 (2012).
5. Parkinson Study Group, The safety and tolerability of a mixed lineage kinase inhibitor (CEP-1347) in PD. *Neurology* **62**, 330–332 (2004).
6. Parkinson Study Group PRECEPT Investigators, Mixed lineage kinase inhibitor CEP-1347 fails to delay disability in early Parkinson disease. *Neurology* **69**, 1480–1490 (2007).
7. D. F. Marker *et al*., The new small-molecule mixed-lineage kinase 3 inhibitor URMC-099 is neuroprotective and anti-inflammatory in models of human immunodeficiency virus-associated neurocognitive disorders. *J. Neurosci.* **33**, 9998–10010 (2013).
8. K. Tomita *et al*., Mixed-lineage kinase 3 pharmacological inhibition attenuates murine nonalcoholic steatohepatitis. *JCI Insight* **2**, e94488 (2017).
9. T. Kiyota *et al*., URMC-099 facilitates amyloid-β clearance in a murine model of Alzheimer's disease. *J. Neuroinflammation* **15**, 137 (2018).
10. M. J. Bellizzi *et al*., The mixed-lineage kinase inhibitor URMC-099 protects hippocampal synapses in experimental autoimmune encephalomyelitis. *eNeuro* **5**, ENEURO.0245-18.2018 (2018).
11. S. Das *et al*., Human epidermal growth factor receptor 2 (HER2) impedes MLK3 kinase activity to support breast cancer cell survival. *J. Biol. Chem.* **290**, 21705–21712 (2015).
12. P. Mishra, S. Senthivinayagam, V. Rangasamy, G. Sondarva, B. Rana, Mixed lineage kinase-3/JNK1 axis promotes migration of human gastric cancer cells following gastrin stimulation. *Mol. Endocrinol.* **24**, 598–607 (2010).
13. Si. Hirai *et al*., MST/MLK2, a member of the mixed lineage kinase family, directly phosphorylates and activates SEK1, an activator of c-Jun N-terminal kinase/stress-activated protein kinase. *J. Biol. Chem.* **272**, 15167–15173 (1997).
14. K. A. Gallo, G. L. Johnson, Mixed-lineage kinase control of JNK and p38 MAPK pathways. *Nat. Rev. Mol. Cell Biol.* **3**, 663–672 (2002).
15. T. Crompton, K. C. Gilmour, M. J. Owen, The MAP kinase pathway controls differentiation from double-negative to double-positive thymocyte. *Cell* **86**, 243–251 (1996).
16. P. Delgado, E. Fernández, V. Dave, D. Kappes, B. Alarcón, CD3delta couples T-cell receptor signalling to ERK activation and thymocyte positive selection. *Nature* **406**, 426–430 (2000).
17. L. Weiss *et al*., Regulation of c-Jun NH(2)-terminal kinase (Jnk) gene expression during T cell activation. *J. Exp. Med.* **191**, 139–146 (2000).
18. R. Noubade *et al*., Activation of p38 MAPK in CD4 T cells controls IL-17 production and autoimmune encephalomyelitis. *Blood* **118**, 3290–3300 (2011).
19. T. Suddason, S. Anwar, N. Charlaftis, E. Gallagher, T-cell-specific deletion of Map3k1 reveals the critical role for Mekk1 and Jnks in Cdkn1b-dependent proliferative expansion. *Cell Rep.* **14**, 449–457 (2016).
20. Z. Borovsky, G. Mishan-Eisenberg, E. Yaniv, J. Rachmilewitz, Serial triggering of T cell receptors results in incremental accumulation of signaling intermediates. *J. Biol. Chem.* **277**, 21529–21536 (2002).
21. C. Dong *et al*., JNK is required for effector T-cell function but not for T-cell activation. *Nature* **405**, 91–94 (2000).
22. C. Dong *et al*., Defective T cell differentiation in the absence of Jnk1. *Science* **282**, 2092–2095 (1998).
23. D. Conze *et al*., c-Jun NH(2)-terminal kinase (JNK)1 and JNK2 have distinct roles in CD8(+) T cell activation. *J. Exp. Med.* **195**, 811–823 (2002).
24. C. Schwechheimer, M. J. Kuehn, Outer-membrane vesicles from gram-negative bacteria: Biogenesis and functions. *Nat. Rev. Microbiol.* **13**, 605–619 (2015).
25. J. Colgan *et al*., Cyclophilin A regulates TCR signal strength in CD4+ T cells via a proline-directed conformational switch in Itk. *Immunity* **21**, 189–201 (2004).
26. H. Makino *et al*., A selective inhibition of c-Fos/activator protein-1 as a potential therapeutic target for intervertebral disc degeneration and associated pain. *Sci. Rep.* **7**, 16983 (2017).
27. K. Takahashi, C. Uchida, R. W. Shin, K. Shimazaki, T. Uchida, Prolyl isomerase, Pin1: New findings of post-translational modifications and physiological substrates in cancer, asthma and Alzheimer's disease. *Cell. Mol. Life Sci.* **65**, 359–375 (2008).
28. J. W. Putney, Calcium signaling: Deciphering the calcium-NFAT pathway. *Curr. Biol.* **22**, R87–R89 (2012).
29. S. Klein-Hessling *et al*., NFATc1 controls the cytotoxicity of CD8$^+$ T cells. *Nat. Commun.* **8**, 511 (2017).
30. S. Dushyanthen *et al*., Agonist immunotherapy restores T cell function following MEK inhibition improving efficacy in breast cancer. *Nat. Commun.* **8**, 606 (2017).
31. S. Gross, R. Rahal, N. Stransky, C. Lengauer, K. P. Hoeflich, Targeting cancer with kinase inhibitors. *J. Clin. Invest.* **125**, 1780–1789 (2015).